High speed imaging chopper polarimetry

Roy M. Matchko[*] and Grant R. Gerhart[**]

*Battelle Scientific Services Program, 1307 W.Remuda Way, Payson, AZ 85541, 928-472-3179,

rmatchko@msn.com

**US Army Tank-Automotive Research Development and Engineering Center, Warren, MI 48397,

585-574-8634, grant.gerhart@us.army.mil

Report Documentation Page

Form Approved
OMB No. 0704-0188

1. REPORT DATE	2. REPORT TYPE	3. DATES COVERED
01 SEP 2007	**N/A**	**-**

4. TITLE AND SUBTITLE	5a. CONTRACT NUMBER
High speed imaging chopper polarimetry	5b. GRANT NUMBER
	5c. PROGRAM ELEMENT NUMBER
6. AUTHOR(S)	5d. PROJECT NUMBER
Roy M. Matchko; Grant R. Gerhart	5e. TASK NUMBER
	5f. WORK UNIT NUMBER
7. PERFORMING ORGANIZATION NAME(S) AND ADDRESS(ES)	8. PERFORMING ORGANIZATION REPORT NUMBER
US Army RDECOM-TARDEC 6501 E 11 Mile Rd Warren, MI 48397-5000	**16981**
9. SPONSORING/MONITORING AGENCY NAME(S) AND ADDRESS(ES)	10. SPONSOR/MONITOR'S ACRONYM(S)
	TACOM/TARDEC
	11. SPONSOR/MONITOR'S REPORT NUMBER(S)
	16981

12. DISTRIBUTION/AVAILABILITY STATEMENT
Approved for public release, distribution unlimited

13. SUPPLEMENTARY NOTES
Published in Opt. Engl, Vol.47, 016001 (2008)

14. ABSTRACT

15. SUBJECT TERMS

16. SECURITY CLASSIFICATION OF:			17. LIMITATION OF ABSTRACT	18. NUMBER OF PAGES	19a. NAME OF RESPONSIBLE PERSON
a. REPORT	b. ABSTRACT	c. THIS PAGE			
unclassified	**unclassified**	**unclassified**	**SAR**	**37**	

Abstract

The Stokes method provides a seminal method for the determination of a state of polarization of a beam of light using measurable quantities. This paper presents a methodology for the rapid acquisition of the four Stokes parameters. We have been able to acquire images at the rate of 500 images per second using a high speed video camera. Using the high speed video camera, an optical chopper, a computer system containing a frame grabber and software to coordinate all elements of the system, the four Stokes parameters have been acquired in 6 milliseconds. Included in this paper is a description of all elements of the system, the calibration of the camera and polarization elements, the design of the optical chopper polarimeter, and corrections related to rotation of polarization elements during exposure. A discussion of errors includes variations in pixel sensitivity, ill-conditioning of the Stokes parameters, aperture clipping, quasi-monochromatic approximation and variations in the Stokes parameters during data acquisition. Validation and testing of the methodology includes a comparison of empirical and theoretical skylight polarization parameters and values related to known, rapidly changing polarization states using several different bandwidth filters.

Keywords: polarization, polarimetry, Stokes parameters, image acquisition, image processing, skylight

Introduction

The Stokes methodology is a seminal method to determine the polarization state of light[1]. This procedure requires four independent intensity measurements to characterize the most general case for elliptically polarized electromagnetic waves. Each measurement corresponds to one of four distinct optical filter arrangements. The Stokes parameters in this paper are defined as S_0, S_1, S_2 and S_3.

Temporal and spatial registration errors are two major sources of error prevalent in all 4-Stokes parameter measurement systems. They may occur because the scene changes temporally during the data acquisition time interval. These non-stationary effects can alter the four intensity measurements and cause significant errors in the final determination of the Stokes parameters. These effects can be important in scenes where changing sun position or cloud conditions produce rapid changes in ambient illumination. In laboratory experiments, variations in temperature, pressure, density or concentration variations can cause similar effects. Spatial registration problems occur when the scene shifts in angular orientation relative to the camera during the image recording process. For example, if four spatially adjacent camera systems simultaneously record imagery associated with a different polarization filter, each image will record a slightly different perspective of the original scene. This technique would reduce temporal registration errors, but would potentially increase errors due to spatial misregistration. These four images would have to be remapped or warped in order to correct for parallax effects. In single camera systems background vibration, noise and unstable platforms can also produce spatial misregistration of imagery. Our experience has been that these effects can be eliminated or controlled using careful experimental procedures. Temporal registration problems, however, are typically much more difficult to correct.

Target discrimination and object recognition are major objectives in our pursuit of faster imaging polarimeters. Pseudo ellipticity, which can be produced by temporal registration errors, produces false signatures which defeat the main objectives. The authors have developed an imaging chopper polarimeter to decrease the time intervals between images and automate the image acquisition process. This system acquires 4-Stokes parameter imagery using a high-speed, digital, video camera. It reduces the total data acquisition time from 30 seconds in our earlier COTS digital still camera polarimeter[2] and from 0.6 seconds using our rotating retarder apparatus and COTS digital camcorder[3] to 0.006 seconds in our new imaging chopper polarimeter.

The Optical Chopper Polarimeter

Figure 1 shows the Stokes filter wheel used to acquire the four Stokes parameters. It consists of five trigger holes; three linear polarizers, identified by I(0,0,0), I(0,90,0), and I(0,45,0); one circular polarizer, identified by I(90,45,ε) and an opaque reference screen. Figure 2 shows the components of the optical chopper polarimeter and the connections between them.

The frequency of the Stokes filter wheel is selected from the optical chopper controller (Scitec 300 CD) and sent to the Stokes filter wheel via connection 1. The computer is used to select the mode of operation (e.g., internal/ external triggering, etc.), the region of interest (ROI, the pixel area to be used in the exposure), and the exposure time of the video camera (Dalsa 1M75). These selections are transmitted to the video camera via connection 4.

Signals are sent from the infrared sensor to the optical chopper controller via connection 2 whenever a trigger hole passes between the infrared transmitter and receiver. The optical chopper controller sends a signal (e.g., a 5-volt TTL voltage) to the frame grabber (BitFlow R64) via connection 3 whenever the optical chopper controller receives a signal from the infrared sensor.

The frame grabber sends a triggering command to the video camera via connection 4 whenever the optical chopper receives a signal from the infrared sensor. The video camera sends the captured image to the frame grabber via connection 5 when the shutter of the video camera closes. Computer software (StreamPix) formats (e.g., bmp, jpg, tif, etc.) the raw data from the frame grabber and saves it to ram memory or to the hard drive of the computer.

Calibration

Calibration of the Video Camera

Because the Stokes parameters use intensity measurements or a parameter proportional to intensity and the output from the video camera is in RGB gray scale values, a relationship must be obtained between the RGB gray scale values and the intensity. A calibration method for obtaining this relationship is to pass a beam of unpolarized light through neutral density filters of different optical densities. Curve-fitting yields RGB gray scale values as a function of optical density (OD). The best curve-fit was obtained using the general quadratic equation

$$A x^2 + B xy + C y^2 + D x + E y + F = 0 \qquad (1)$$

Using x to represent OD and y to represent RGB gray scale values, Eq. (2) gives OD as a function of RGB gray scale values, where A, B, C, D, E and F are the coefficients of Eq. (1).

$$x = \frac{-(By + D) + \sqrt{(By + D)^2 - 4A(Cy^2 + Ey + F)}}{2A} \tag{2}$$

The calibration curve obtained for the Dalsa 1M75, when unpolarized incident light was transmitted through a green Kodak #58 broadband (100 nm) filter, was a hyperbola. Relative intensities, I, are obtained from optical densities as given in

$$I = 10^{-OD} \tag{3}$$

Calibration of the Circular Polarizer

A circular polarizer is used to obtain the fourth Stokes parameter and is identified in Fig. 2 as $I(90,45,\varepsilon)$; ε is the phase difference of the two orthogonal components E_x and E_y of the electric vector transmitted through the circular polarizer.

A circular polarizer consists of a linear polarizer and a quarter-wave retarder. The transmission axis of the linear polarizer is oriented at a 45° angle to the fast axis of the retarder. The phase difference, ε, can be determined empirically by positioning a linear polarizer in front of the circular polarizer, as shown in Fig. 3. In order for the circular polarizer to be used in determining the fourth Stokes parameter, the incident light must first be transmitted through the quarter-wave retarder and then through the linear polarizer. The empirical ε-values are obtained when $\alpha = 0°$ and 45°, $\beta = 0°$ and $\theta = -45°$.

Using Mueller matrices[4], the intensity of the light transmitted through P1, R and P2 of Fig. 3, $I(\alpha,\beta,\theta,\varepsilon)$, is obtained from

$$I(\alpha,\beta,\theta,\varepsilon) = I_0 \{\cos^2 (\alpha+\theta-2\beta) + \sin 2(\alpha-\beta) \sin (\theta-\beta) \cos (\theta-\beta) (1 + \cos \varepsilon)\} \quad (4)$$

where I_0 is the intensity of the incident light on P1.

Inserting $\alpha = 0°$, $\beta = 0°$ and $\theta = -45°$ and $\alpha = 45°$, $\beta = 0°$ and $\theta = -45°$ into Eq. (4) and solving for ε yields

$$\varepsilon = \text{acos}\left[1 - \frac{I(45,0,-45,\varepsilon)}{I(0,0,-45,\varepsilon)}\right] \quad (5)$$

To obtain empirical ε-values, collimated white light was transmitted through a frosted glass plate and then through different narrowband (10 nm) filters. Using a Minolta LS 100 luminance meter to record data and Eq. (5), the phase difference of the 3M circular polarizer as a function of wavelength, λ, is

$$\varepsilon = -2.52 \text{ X } 10^{-06} \lambda^2 + 5.27 \lambda - 0.53 \quad (6)$$

Figure 4 shows ε as a function of wavelength, λ.

Calibration of the Stokes Filter Wheel

The four polarization elements used to obtain the four Stokes parameters must have the same optical density or calculations of these parameters must incorporate compensation for differences. Using the Dalsa 1M75 camera, uniform, unpolarized, collimated light was transmitted through each element of the Stokes filter wheel (Fig. 1) and the optical density for each of the four elements was obtained from Eq.

(2) and the relative intensities from Eq. (3). Each of the four relative intensities is divided by the largest of the four relative intensities to obtain a compensation ratio (CR) for each element. Each of the empirical relative intensities is multiplied by its associated CR.

Corrections Due to Rotation During Exposure

The intensity of polarized light transmitted first through a quarter-wave retarder and then through a linear polarizer, as shown in Fig. 5, can be obtained through the use of Mueller matrices[4] and is given in Eq. (7).

$$I(\Omega, \theta, \varepsilon) = 0.5 \{\mathbf{S_0} + [\cos 2\theta - \sin 2\Omega \sin 2(\Omega - \theta) (1 - \cos \varepsilon)]\ \mathbf{S_1} +$$
$$[\sin 2\Omega \cos 2(\Omega - \theta) - \cos 2\Omega \sin 2(\Omega - \theta) \cos \varepsilon\ ]\ \mathbf{S_2} - \sin 2(\Omega - \theta) \sin \varepsilon\ \mathbf{S_3}\} \quad (7)$$

$I(\Omega, \theta, \varepsilon)$ is the relative intensity for a particular set of angles Ω, θ, and ε, where ε is the phase difference produced by the retarder; S_0, S_1, S_2, and S_3 are the Stokes parameters of the incident polarized light.

Three of the apertures in the Stokes filter wheel are fitted with linear polarizers. Since retarders are not present in these apertures, Ω and ε are zero. Equation (8) gives the general equation for the intensity of the light after transmission through any of the three linear polarizers in the Stokes filter wheel.

$$I_{LP} = I(0, \theta, 0) = 0.5 [\mathbf{S_0} + (\cos 2\theta)\ \mathbf{S_1} + (\sin 2\theta)\ \mathbf{S}_2] \quad (8)$$

The fourth chopper blade aperture contains a left circular polarizer with its quarter-wave retarder facing the incident light and its linear polarizer adjacent to the camera. Since the fast axis of the retarder is positioned 45 degrees from the transmission axis of the linear polarizer, the general equation for the intensity, I_4, of the light transmitted through the circular polarizer is given by

$$I_4 = I(\theta + \pi/4, \theta, \varepsilon) = 0.5\,[\mathbf{S_0} + (\cos 2\theta \cos \varepsilon)\,\mathbf{S_1} + (\sin 2\theta \cos \varepsilon)\,\mathbf{S_2} - \sin \varepsilon\,\mathbf{S_3}] \quad (9)$$

The set of angles associated with each aperture of a stationary Stokes filter wheel, when associated trigger holes are positioned at the sensor, is given in Eq. (10).

$$(\Omega, \theta, \varepsilon)_1 = (0, 0, 0),\ (\Omega, \theta, \varepsilon)_2 = (0, 90°, 0),\ (\Omega, \theta, \varepsilon)_3 = (0, 45°, 0),$$
$$\text{and } (\Omega, \theta, \varepsilon)_4 = (90°, 45°, \varepsilon). \quad (10)$$

Using Eq. (10) in Eqs. (8) and (9) and solving for the Stokes parameters yields

$$S_0 = I_1 + I_2 \qquad S_1 = I_1 - I_2 \qquad S_2 = 2\,I_3 - S_0 \qquad S_3 = [S_0 + \cos \varepsilon\, S_2 - 2\,I_4]/\sin \varepsilon \quad (11)$$

However, since the apertures rotate through an angle δ during the exposure, as shown in Fig. 6, the actual intensities recorded by the camera are the average intensities, represented by "*", which can be determined from the average value of a function.

If a linear polarizer rotates through an angle δ during the acquisition of I_{LP}, then using Eq.8, the measured value of I_{LP}, corresponding to I_1, I_2 or I_3, is obtained from Eq. (12).

$$I^*_{LP} = \frac{1}{2}\left[S_0 + \frac{S_1}{\delta} \int_{\theta}^{\theta+\delta} \cos 2\theta \, d\theta + \frac{S_2}{\delta} \int_{\theta}^{\theta+\delta} \sin 2\theta \, d\theta \right] \quad (12)$$

Integration of Eq. (12) yields

$$I^*_{LP} = \tfrac{1}{2} \{\mathbf{S_0} + (1/2\delta) [\sin 2(\theta+\delta) - \sin 2(\theta)] \mathbf{S_1} - (1/2\delta) [\cos 2(\theta+\delta) - \cos 2(\theta)] \mathbf{S_2}\} \quad (13)$$

If the circular polarizer rotates through an angle δ during the acquisition of I_4, then using Eq. 9, the measured value of I_4 is obtained from Eq. (14).

$$I^*_4 = \frac{1}{2}\left[S_0 + \frac{S_1 \cos\varepsilon}{\delta} \int_{\theta}^{\theta+\delta} \cos 2\theta \, d\theta + \frac{S_2 \cos\varepsilon}{\delta} \int_{\theta}^{\theta+\delta} \sin 2\theta \, d\theta - \frac{S_3 \sin\varepsilon}{\delta} \int_{\theta}^{\theta+\delta} d\theta \right] \quad (14)$$

Integration of Eq. (14) yields

$$I^*_4 = \tfrac{1}{2} \{\mathbf{S_0} + [\cos \varepsilon/2\delta] [\sin (2\theta + 2\delta) - \sin (2\theta)] \mathbf{S_1} - [\cos \varepsilon/2\delta] [\cos (2\theta + 2\delta) - \cos (2\theta)] \mathbf{S_2} - \sin \varepsilon \mathbf{S_3}\} \quad (15)$$

Using Eq. (10) in Eqs. (13) and (15) yields

$$I^*_1 = I^*(0,0,0,\delta) = \tfrac{1}{2} [\mathbf{S_0} + (\sin \delta/\delta) (\cos \delta \mathbf{S_1} + \sin \delta \mathbf{S_2})]$$

$$I^*_2 = I^*(0,90,0,\delta) = \tfrac{1}{2} [\mathbf{S_0} - (\sin \delta/\delta) (\cos \delta \mathbf{S_1} + \sin \delta \mathbf{S_2})]$$

$$I^*_3 = I^*(0,45,0,\delta) = \tfrac{1}{2} [\mathbf{S_0} - (\sin \delta/\delta) (\sin \delta \mathbf{S_1} - \cos \delta \mathbf{S_2})]$$

$$I_4^* = I^*(90,45,\varepsilon,\delta) = \tfrac{1}{2} [\mathbf{S_0} - (\cos \varepsilon \sin \delta/\delta) (\sin \delta \mathbf{S_1} - \cos \delta \mathbf{S_2}) - \sin \varepsilon \mathbf{S_3}] \quad (16)$$

Solving Eq. (16) for the four Stokes parameters yields

$\mathbf{S_0} = (I^*_1 + I^*_2)$

$\mathbf{S_1} = (\delta/\sin\delta)\,[(\sin\delta + \cos\delta)\, I^*_1 + (\sin\delta - \cos\delta)\, I^*_2 - 2\sin\delta\, I^*_3]$

$\mathbf{S_2} = (\delta/\sin\delta)\,[(\sin\delta - \cos\delta)\, I^*_1 - (\sin\delta + \cos\delta)\, I^*_2 + 2\cos\delta\, I^*_3]$

$\mathbf{S_3 = [S_0} + \cos\varepsilon\,(2\, I^*_3 - \mathbf{S_0)} - 2\, I_4^*]/\sin\varepsilon$ (17)

Note that both S_0 and S_3 are independent of δ, hence, S_0 and S_3 are rotationally invariant! Also, as δ approaches zero, $\delta/\sin\delta$ approaches one and Eq. (17) reduces to Eq. (11).

The degree of polarization, P, the polarization azimuth angle, ψ, and the polarization ellipticity angle, χ, given in Eq. (18), are obtained from the Stokes parameters given in Eq. (17).

$$P = \frac{\sqrt{S_1^{\,2} + S_2^{\,2} + S_3^{\,2}}}{S_0} \qquad \tan 2\psi = \frac{S_2}{S_1} \qquad \sin\ 2\chi = \frac{S_3}{\sqrt{S_1^{\,2} + S_2^{\,2} + S_3^{\,2}}} \tag{18}$$

Aperture Clipping

Aperture clipping occurs when part of an aperture of the Stokes filter moves out of the field of view of the camera during exposure. This phenomenon is especially prominent at high image rates when the exposure time is too long.

Figure 7 shows the dimensions of an aperture of the Stokes filter wheel. Aperture clipping begins when the angular rotation of the chopper blade, δ, exceeds 18° during exposure. During exposure, the maximum amount of rotation that can occur for a single pixel is approximately 65°. Since the elements

of the Stokes filter wheel rotate around a circle with constant speed, and 5 images are acquired in one revolution of the chopper blade

$$|\delta| = 2\,\pi\,f\,t\ (\text{rad}) = 72\,F\,t\ (\text{deg}) \qquad (19)$$

where F is the camera image rate and t is the exposure time in seconds. The maximum image rate attainable with the Scitec 300 CD, operating with 5 apertures, is 500 images per second. The angular rotation of the Stokes filter wheel, using 500 images per second and an exposure time of 0.5 ms, is 18°; just avoiding aperture clipping.

Errors

Photosite Sensitivity Variations

Although flat frames help in the correction of photosite sensitivity variations in the Dalsa 1M75 video camera, the sensitivity of each pixel can vary with intensity by as much as 10%, as shown in Fig. 10. Figure 10 gives the sensitivity ratio for individual pixels in selected rows and column #40 of the CMOS image sensor for different incident light intensities. The sensitivity ratio is the ratio of a pixel value in the flat frame and the average pixel value of the entire flat frame. The data associated with Fig. 10 was obtained by transmitting a uniform, collimated, white light beam through different neutral density filters. Fluctuations in pixel sensitivity, camera noise, line voltage fluctuations, mechanical vibrations and image rate all contribute to errors in the calculation of the Stokes parameters.

Ill-conditioning of Stokes Parameters

The Stokes parameters are prone to giving false polarization parameters when low intensities are involved in their calculation or when they are near or equal to zero; the errors in calculating the P, ψ or χ values can be very significant. ψ-values are undefined for circularly polarized light and are ill-conditioned for χ-values near ±458.

Conversely, errors in the χ-values can be very small, especially for high degrees of polarization (P ~ 1.00). According to Eq. (18), when P = 1.00, χ-values depend solely on S_3, which is independent of rotation of the chopper blade during exposure and hence is rotationally invariant.

Quasi-Monochromatic Approximation

Light is considered to be quasi-monochromatic when the wavelength range is small compared to the mean wavelength.[5] The set of four Stokes parameters given in Eqs. (11) and (17) are generally considered to be valid for only quasi-monochromatic light.[6] Figure 8 shows the relative transmission through three different filters as a function of the incident wavelength. The primary purpose of the "hot mirror" is to eliminate the transmission of infrared radiation. The Kodak #58 filter is a broadband green filter with a bandwidth of approximately 100 nm. The Oriel #56561 filter is a narrowband green filter with a bandwidth of approximately 10 nm. The Oriel #56561 filter is the only filter shown in Fig. 8 that satisfies the quasi-monochromatic condition. However, it will be shown in the studies that follow that the use of the broadband Kodak #58 filter and the "hot mirror" filter produce similar polarization parameters as obtained from the narrowband Oriel #56561 filter.

The phase difference, ε, of the circular polarizer used in the Stokes filter wheel is wavelength dependent, as Eq. (6) and Fig. 4 illustrate; hence, the fourth Stokes parameter, expressed in Eqs. (11) and (17), is also wavelength dependent. Since Eq. (6) can only accommodate one specific input wavelength, errors are introduced into polarization parameters dependent on S_3; namely, P and χ. The polarization azimuth angles are completely independent of the phase difference of the circular polarizer.

Although ε and λ are not related linearly throughout the visible spectrum, they are nearly so within a 100 nm bandwidth (see Fig. 4). Therefore, to a good approximation, the wavelength corresponding to the average value of ε for a selected 100 nm bandwidth is the one corresponding to the midpoint of the bandwidth[2].

Three separate studies, using each of the three filters shown in Fig. 8, were used to test and validate the quasi-monochromatic approximation. Each study collected 500 images from the Dalsa 1M75 video camera. Since the image rate used for each study was 500 images/sec and five consecutive images are required to determine the Stokes parameters (four polarization images plus a blank reference image), 100 different polarization forms were used in the analysis of each study.

An exposure time of 0.5 ms was used to avoid aperture clipping during exposure. According to Eq. (19) and Fig. 7, the combination of 500 images/sec and an exposure time of 0.5 ms produces 18 degrees of rotation for each filter wheel aperture during exposure; hence aperture clipping is avoided. Matlab scripts are used to calculate the empirical polarization parameters. Equation (17) is used to correct for rotation during exposure.

A region of interest (ROI) of 256 X 256 pixels was required to achieve 500 images/sec from the Dalsa 1M75 video camera. Each and every polarization parameter, in all three studies, was obtained from the average value of a cropped 100 X 100 pixel area.

Rapidly changing, known polarization forms were obtained from a fixed linear polarizer and a rotating quarter-wave retarder, as shown in Fig. 9. In the present studies, the linear polarizer is fixed in a horizontal position and the quarter-wave retarder is rotated at 25 RPMs with a precision motor. This configuration produces the input source to the imaging chopper polarimeter.

Equations for the Stokes parameters incident on the Stokes filter wheel are obtained from the use of Fig. 9 and Mueller matrices and are given in Eq. (20) for the case $\alpha = 0$.

$$S_0 = 1 \quad S_1 = \cos^2 2\beta + \sin^2 2\beta \cos\sigma \quad S_2 = \sin 2\beta \cos 2\beta (1 - \cos\sigma) \quad S_3 = \sin 2\beta \sin\sigma \qquad (20)$$

Since the retarder is transparent and rotating when data acquisition begins, a method must be described to identify the position of the fast axis of the retarder when the first image is captured. The method adopted in these studies uses Eq. (20) with $\beta = 0$ to identify this position. When $\beta = 0$, $S_1 = 1$, $S_2 = 0$; and $S_3 = 0$. Since a Matlab script generates all of the empirical Stokes parameters, it is easy to identify that image containing $\beta = 0$. Since the retarder rotates at 25 RPM (150°/sec) and the image rate is 500 images/sec, there are 0.3 degrees of rotation of the fast axis of the retarder between consecutive images. Theoretical polarization parameters P, ψ and χ are calculated from Eq. (18).

Results of the Quasi-Monochromatic Study

Figure 11 compares the empirical and theoretical polarization parameters P, ψ and χ for each of the three filters. Figure 12 compares the differences (Δ) between the empirical and theoretical polarization parameters P, ψ and χ by superimposing the results from the three color filters.

The Polarization Azimuth Angle

The polarization azimuth angle (ψ) is calculated from S_1 and S_2, as shown in Eq. (18). The largest ψ-value errors in this study, as seen in Fig. 12b, occur near $\beta = \pm 45°$. Referring to Eq. (20), the theoretical value for S_2 is zero when $\beta = \pm 45°$; accounting for the larger errors found in Fig. 12b for these orientations of β. Figure 12b clearly shows that deviations from the quasi-monochromatic approximation do not affect the ψ-values, they are independent of the incident wavelength. Except for the case of $\beta \cong \pm 45°$, Fig. 12b shows that the errors in the ψ-values are less than 4° for all visible wavelengths . **Note:** The polarization azimuth angle is undefined for circular polarization ($\alpha = 0°$, $\beta = \pm 45°$ and $\varepsilon = 90°$).

The Polarization Ellipticity Angle

The polarization ellipticity angle (χ) is calculated from Eq. (18). For normalized Stokes parameters, which are used exclusively throughout this study, the denominator of χ is the degree of polarization, P. Since the incident light on the Stokes filter wheel is completely polarized, the theoretical P-value is P = 1.0. Therefore, the theoretical χ-value depends solely on S_3 and is independent of the other Stokes parameters. For example, P-value errors have little effect on the empirical χ-value. This is so because

the empirical P-values range from 1.0 to only 1.1; hence, the denominator of χ is not much different than unity and the empirical χ-values depend primarily on S_3. Since S_3 is rotational invariant as the Stokes filter wheel rotates, χ-value errors related to rotation are eliminated. The only errors remaining relate to deviations from the quasi-monochromatic approximation and errors introduced by the CMOS image sensor. With the exception of only a few of the 300 data points, the χ-value errors are all less than 4°, as shown in Fig. 12c. Calculations show that when the empirical RGB gray scale values are changed by ±4 gray values, simulating variation in sensor sensitivity, the χ-value can change by 3°. Therefore, if small variations of RGB gray scale values can account for χ-value discrepancies of 3°, the errors due to deviations from the quasi-monochromatic approximation must be very small.

The Degree of Polarization

The degree of polarization (P) is calculated from Eq. (18). Since $S_0 = 1$ for normalized Stokes parameters, P is just the numerator in Eq. (18). Figure 12a shows that, with the exception of two points out of the 300 plotted points, the largest error in the P-value is 10%; the difference in the empirical and theoretical P-values, for the majority of points, is 6%. The largest errors occur for the narrowband filter, which is not surprising. The narrowband filter has the largest optical density and requires greater incident light intensity than the other filters to produce the same RGB values. The largest intensity available was used in the data acquisition related to the narrowband filter. On the other hand, neutral density filters were used in conjunction with the other two filters in order to prevent over exposure.

Diurnal Skylight Study

The imaging chopper polarimeter was used to acquire diurnal polarization parameters of a small area of skylight. Using an image rate of 500 frames/s and an exposure time of 0.46 ms, empirical values of P, ψ

and χ were acquire from 10:00 to 16:00 at intervals of 15 minutes, during clear skies, at longitude 111° west and latitude 34° north. Empirical values for skylight were obtained from averaging over 30 X 30 pixel areas centered northwest at an altitude of 5°. Figure 13 gives the results for this study.

The Degree of Polarization

The theoretical skylight polarization parameters are obtained using the Rayleigh scattering model. Equation 21 gives a modern version of Lord Rayleigh's theoretical description for skylight polarization[7].

$$P = \frac{\sin^2\Omega}{1+\cos^2\Omega} \tag{21}$$

Ω is the scattering angle in the observation plane containing the incident solar ray, scattering center and observer[8]. Lord Rayleigh assumed the incident, unpolarized light is scattered by small isotropic particles (e.g. air molecules much smaller than the wavelength of light). The scattering angle Ω can be expressed in the more useful earth-horizon coordinate system, using spherical coordinates, as follows:

$$\cos\Omega = \cos\alpha\cos\theta\cos(A-\varphi) + \sin\alpha\sin\theta \tag{22}$$

where α is the altitude of the sun, A is azimuth of the sun, θ is the altitude of the point of observation on the celestial sphere and φ is the azimuth of the point of observation. We use the convention that south corresponds to 0° and west to 90°. The difference between theoretical and empirical P-values The largest difference between the empirical and theoretical ψ-values, as seen in Fig. 13a, is less than 6% between 10:00 and 14:30; a maximum difference of 17% is acquired at 15:00.

The Polarization Azimuth Angle

In a previous paper[9] we derive an equation for the polarization azimuth angle of skylight in the earth-horizon coordinate system, as given Eq. (23).

$$\cos\psi = \frac{\sin\alpha\ \cos\theta - \sin\theta\ \cos\alpha\ \cos(\varphi - \mathrm{A})}{\pm\sqrt{1-\left(\sin\alpha\ \sin\theta + \cos\theta\ \cos\alpha\ \cos(\varphi - \mathrm{A})\right)^2}} \tag{23}$$

where α is the altitude of the sun, A is azimuth of the sun, θ is the altitude of the point of observation on the celestial sphere and φ is the azimuth of the point of observation. The largest difference between the empirical and theoretical ψ-values, as seen in Fig. 13b, is 4.5°.

The Polarization Ellipticity Angle

According to Rayleigh scattering theory, the ellipticity angle, χ, of skylight is zero. The largest difference between the empirical and theoretical χ-values, as seen in Fig. 13c, is 4.3°.

Equations (21) and (23) do not take into account interactions between the incident solar radiation and large atmospheric particles (cloud droplets, ice crystals, aerosols, etc.) and effects due to multiple scattering and molecular anisotropy.

Conclusion

Current use of the optical chopper polarimeter has produced outstanding laboratory results. The difference between empirical and theoretical ψ-values is less than 4°, except for the case of $\beta \cong \pm 45°$, which produced a 10° difference. The difference between empirical and theoretical χ-values is less than 4°. The largest error in the P-values is approximately 10%; however, for the majority of points, the errors are less than 6%. The use of the quasi-monochromatic approximation with broadband filters shows negligible effects on the χ-values and only small effects on the P-values.

Future studies will attempt to further reduce the acquisition time of the four Stokes parameters. Additional studies will use the optical chopper polarimeter in daylight scenes to study non-uniform, natural and man-made targets.

References

1. G.G Stokes, “On the composition and resolution of streams of polarized light from different sources,” Trans. Cambridge Phil. Soc. 9, 399 (1852); *Mathematical and physical papers,* vol. 3 (Cambridge University Press, Cambridge, England, 1901), 233

2. R.M. Matchko and G.R. Gerhart, “Polarization measurements using a comercial off-the-shelf digital camera,” *Opt. Eng.* **44(2),** 023604 (2005).

3. R.M. Matchko and G.R. Gerhart, “Rapid 4-Stokes parameter determination using a motorized rotating retarder,” *Opt. Eng.* **45(09),** 098002 (2006).

4. A. Gerrard and J. M. Burch, *Introduction to Matrix Methods in Optics*, Dover Publications, N. Y., p. 196 (1994.).

5. M. Born and E. Wolf, *Principles of Optics*, 6th ed., New York, p. 264, Pergamon Press, New York (1993).

6. M. Born and E. Wolf, *Principles of Optics*, 6th ed., New York, pp. 554-555, Pergamon Press, New York (1993).

7. M. Born and E. Wolf, *Principles of Optics*, 6th ed., (Pergamon Press, New York, 1993), pp. 652-656.

8. W. J. Humphreys, *Physics of the Air*, (Dover Publications 1964), p. 561.

9. R.M. Matchko and G.R. Gerhart, “Polarization azimuth angle in daylight scenes,” *Opt. Eng.* **44(2),** 028001 (2005).

Figure Captions

Fig. 1 The Stokes filter wheeel.

Fig. 2 The components of the optical chopper polarimeter and the connections between them.

Fig. 3 Apparatus for obtaining the phase difference of a circular polarizer.

Fig. 4 The phase difference of a 3M circular polarizer as a function of wavelength.

Fig. 5 Incident light transmitted through a retarder and a linear polarizer.

Fig. 6 Rotation of the Stokes filter wheel during exposure. If the polarization elements rotate clockwise, then δ is negative.

Fig. 7 The dimensions of a Stokes filter wheel aperture.

Fig. 8 Transmission as a function of wavelength for a "hot mirror" filter, a Kodak #58 filter and an Oriel #56561 filter.

Fig. 9 Components for producing known polarization parameters; the input source to the chopper polarimeter.

Fig. 10 Variations in the sensitivity ratio.

Fig. 11 Comparison of empirical and theoretical polarization parameters. (a, b,c) Degree of Polarization, (d, e, f) Azimuth Angle, (g, h, i) Ellipticity Angle. Input source is a 25 RPM retarder and a fixed horizontal linear polarizer (as shown in Fig.10). Chopper exposure time is 0.5 sec. at 500 frames/sec.

Fig. 12. Comparison of the differences (Δ) between the empirical and theoretical polarization parameters P, ψ and χ by superimposing the results from the three color filters. (a) degree of polarization, P (b) polarization azimuth angle, ψ and (c) polarization ellipticity angle, χ. Input source is

a 25 RPM retarder and a fixed horizontal linear polarizer (as shown in Fig.10). Chopper exposure time is 0.5 sec. at 500 frames/sec.

Fig. 13. Comparison of empirical and theoretical skylight polarization parameters during clear skies. (a) degree of polarization, (b) polarization azimuth angle, (c) polarization ellipticity angle. Chopper exposure time is 0.5 sec. at 500 images/sec.

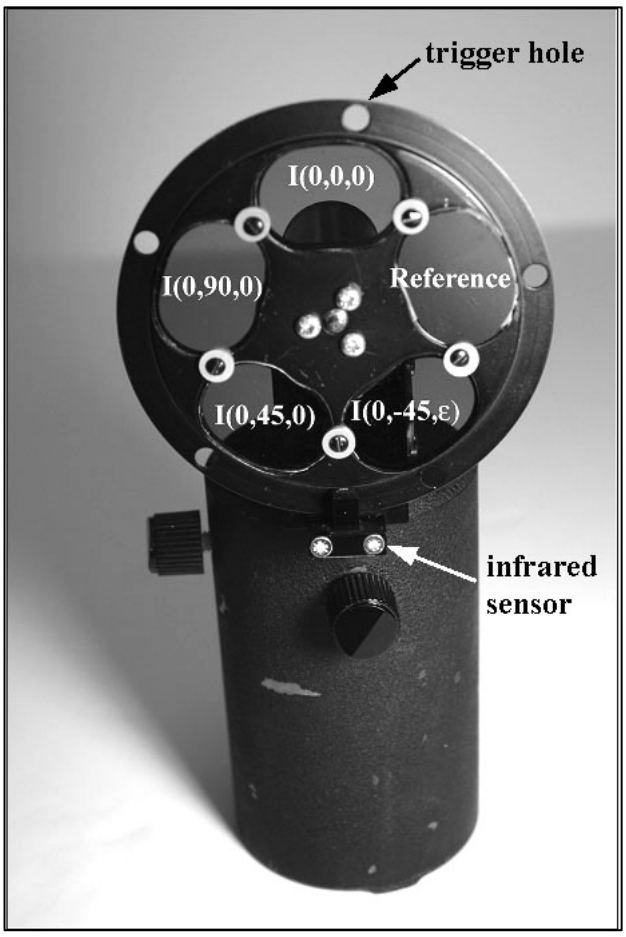
trigger hole
I(0,0,0)
I(0,90,0)
Reference
I(0,45,0)
I(0,-45,ε)
infrared
sensor

Fig. 1

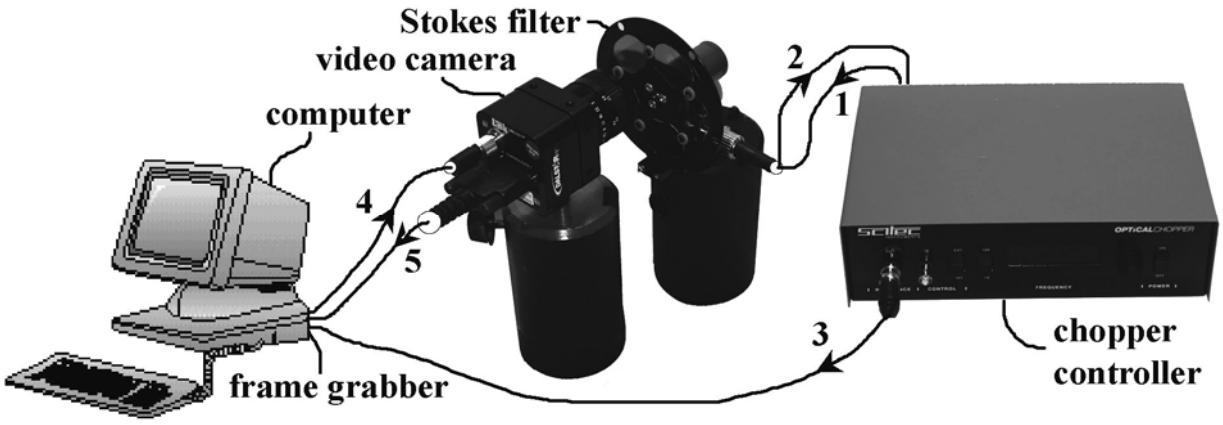
Stokes filter
video camera
computer
2
1
4
5
3
frame grabber
chopper
controller

Fig. 2

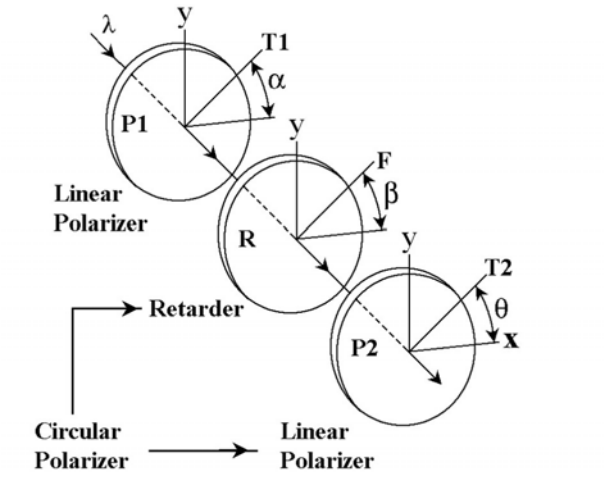
λ
y
T1
α
P1
y
F
β
Linear
Polarizer
R
y
T2
θ
x
P2
Retarder
Circular
Polarizer
Linear
Polarizer

Fig. 3

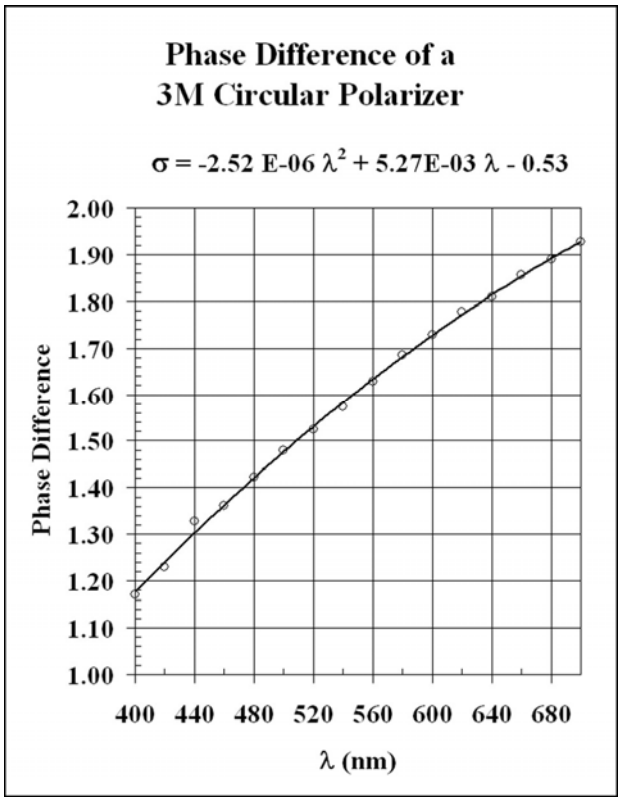
Phase Difference of a
3M Circular Polarizer
σ = -2.52 E-06 λ² + 5.27E-03 λ - 0.53
Phase Difference
2.00
1.90
1.80
1.70
1.60
1.50
1.40
1.30
1.20
1.10
1.00
400 440 480 520 560 600 640 680
λ (nm)

Fig. 4

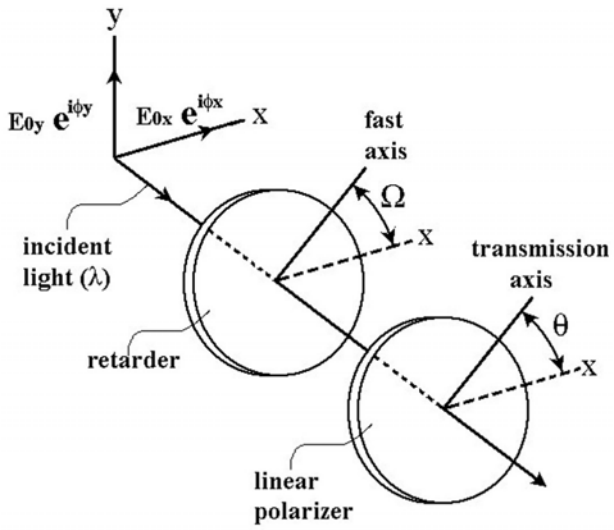
y
E0y e^iϕy
E0x e^iϕx
x
fast
axis
Ω
x
incident
light (λ)
transmission
axis
θ
x
retarder
linear
polarizer

Fig. 5

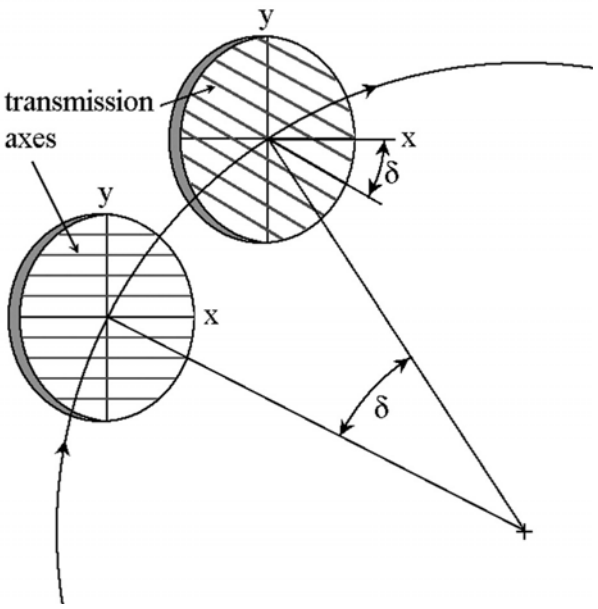

Fig. 6

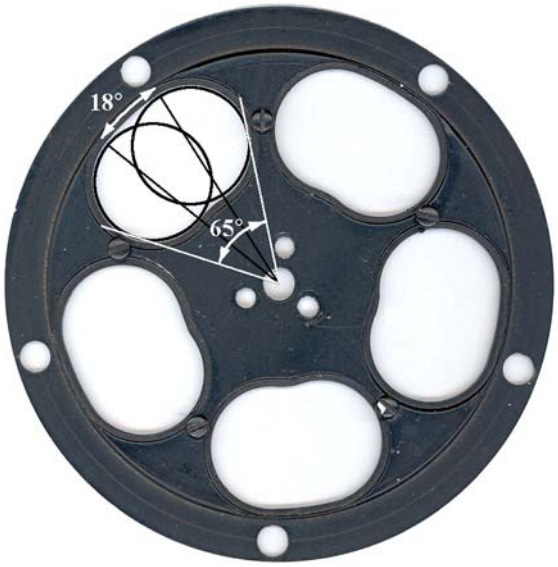

Fig. 7

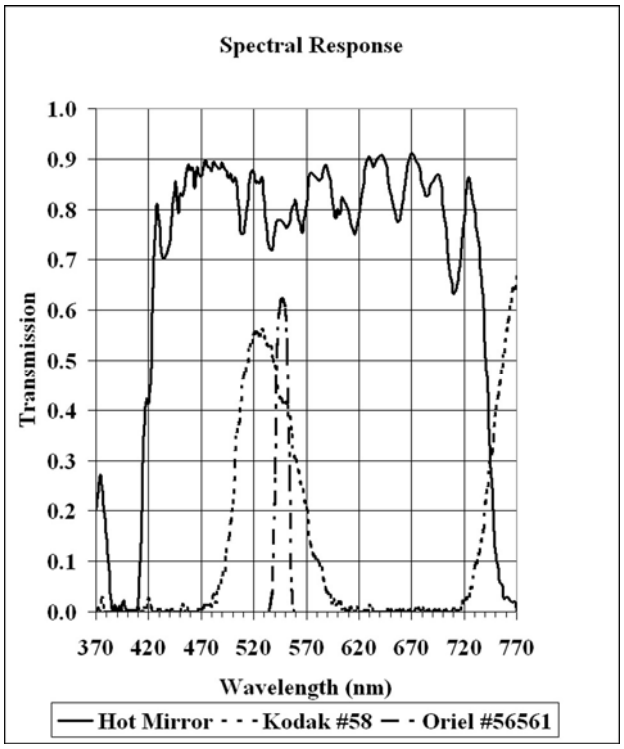
Spectral Response
1.0
0.9
0.8
0.7
0.6
0.5
0.4
0.3
0.2
0.1
0.0
Transmission
370 420 470 520 570 620 670 720 770
Wavelength (nm)
Hot Mirror
Kodak #58
Oriel #56561

Fig. 8

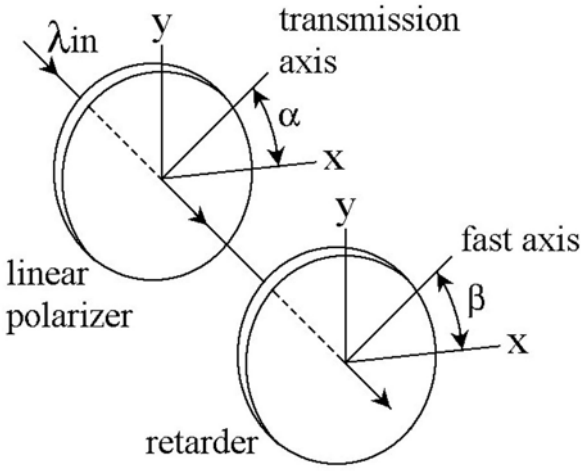
λin
y
transmission
axis
α
x
y
fast axis
β
x
linear
polarizer
retarder

Fig. 9

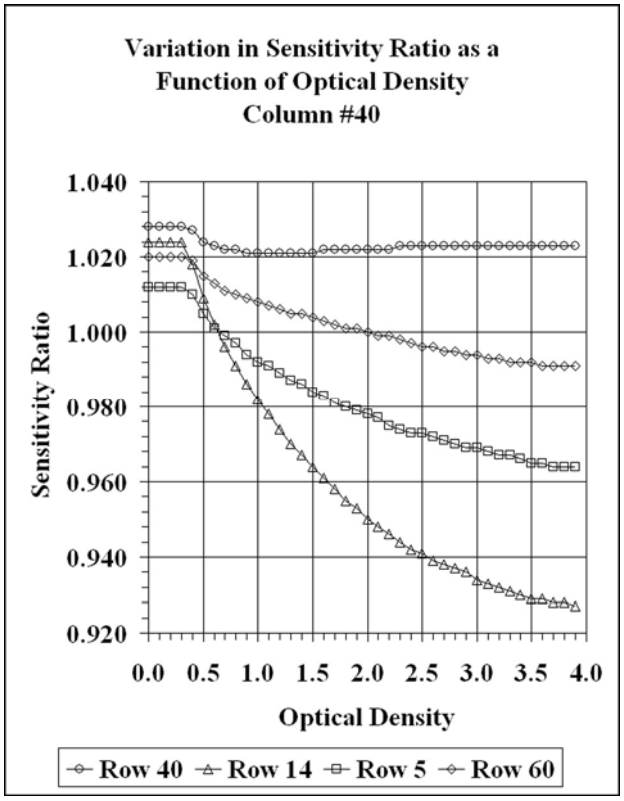
Variation in Sensitivity Ratio as a
Function of Optical Density
Column #40
Sensitivity Ratio
1.040
1.020
1.000
0.980
0.960
0.940
0.920
0.0 0.5 1.0 1.5 2.0 2.5 3.0 3.5 4.0
Optical Density
Row 40
Row 14
Row 5
Row 60

Fig. 10

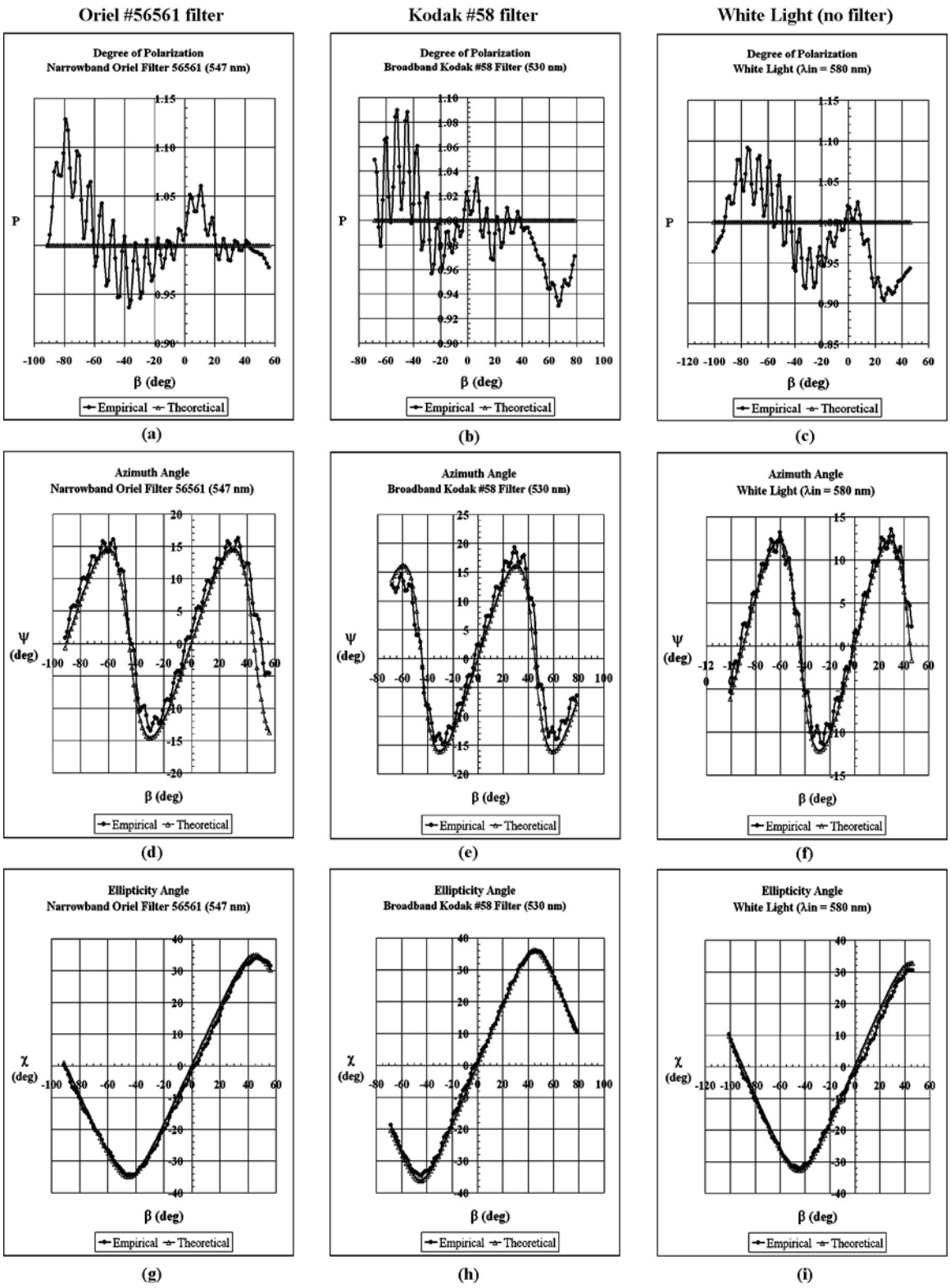
Oriel #56561 filter
Kodak #58 filter
White Light (no filter)
Degree of Polarization
Narrowband Oriel Filter 56561 (547 nm)
Degree of Polarization
Broadband Kodak #58 Filter (530 nm)
Degree of Polarization
White Light (λin = 580 nm)
P
β (deg)
Empirical
Theoretical
(a)
(b)
(c)
Azimuth Angle
Narrowband Oriel Filter 56561 (547 nm)
Azimuth Angle
Broadband Kodak #58 Filter (530 nm)
Azimuth Angle
White Light (λin = 580 nm)
Ψ (deg)
(d)
(e)
(f)
Ellipticity Angle
Narrowband Oriel Filter 56561 (547 nm)
Ellipticity Angle
Broadband Kodak #58 Filter (530 nm)
Ellipticity Angle
White Light (λin = 580 nm)
χ (deg)
(g)
(h)
(i)

Fig. 11

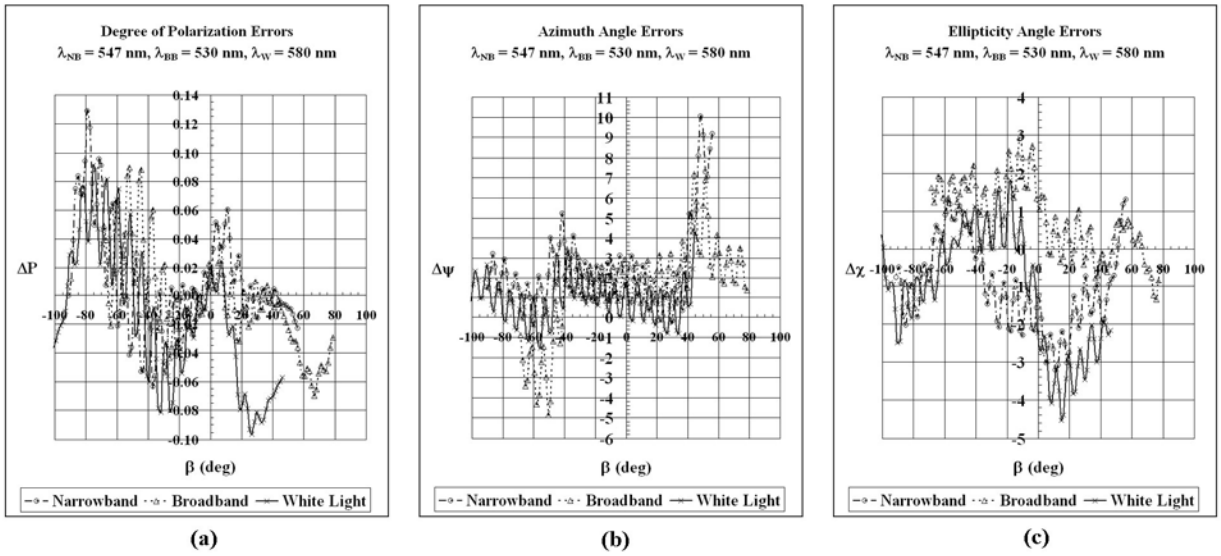
Degree of Polarization Errors
λNB = 547 nm, λBB = 530 nm, λW = 580 nm
ΔP
β (deg)
Narrowband
Broadband
White Light
(a)
Azimuth Angle Errors
λNB = 547 nm, λBB = 530 nm, λW = 580 nm
Δψ
β (deg)
Narrowband
Broadband
White Light
(b)
Ellipticity Angle Errors
λNB = 547 nm, λBB = 530 nm, λW = 580 nm
Δχ
β (deg)
Narrowband
Broadband
White Light
(c)

Fig. 12

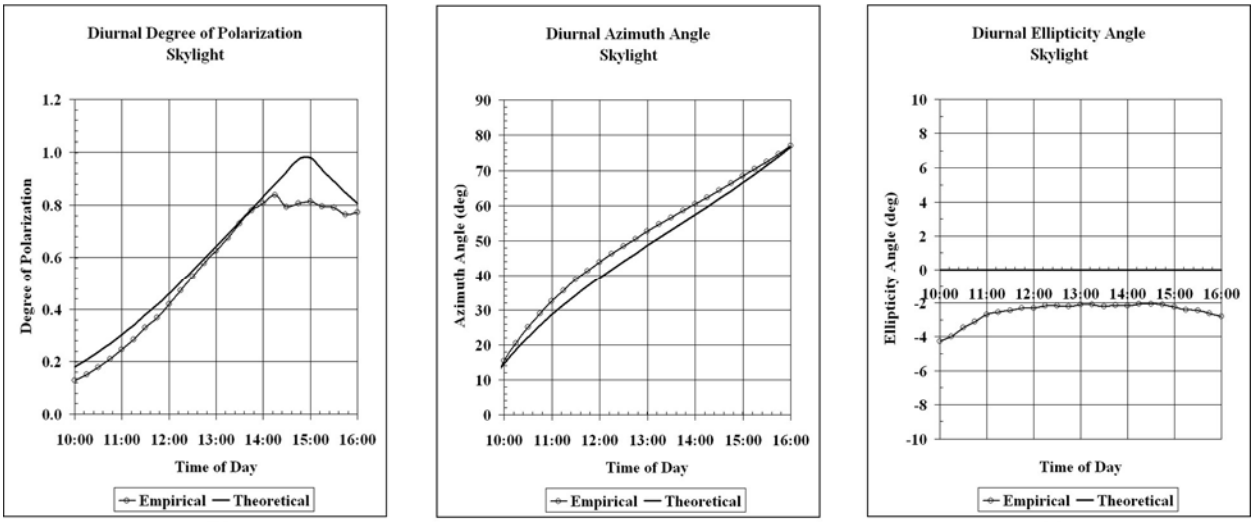
Diurnal Degree of Polarization
Skylight
Degree of Polarization
1.2
1.0
0.8
0.6
0.4
0.2
0.0
10:00 11:00 12:00 13:00 14:00 15:00 16:00
Time of Day
Empirical
Theoretical
(a)
Diurnal Azimuth Angle
Skylight
Azimuth Angle (deg)
90
80
70
60
50
40
30
20
10
0
10:00 11:00 12:00 13:00 14:00 15:00 16:00
Time of Day
Empirical
Theoretical
(b)
Diurnal Ellipticity Angle
Skylight
Ellipticity Angle (deg)
10
8
6
4
2
0
-2
-4
-6
-8
-10
10:00 11:00 12:00 13:00 14:00 15:00 16:00
Time of Day
Empirical
Theoretical
(c)

Fig. 13